Macromolecules

pubs.acs.org/Macromolecules Article

Poly(triazole) Glassy Networks via Thiol-Norbornene Photopolymerization: Structure−Property Relationships and Implementation in 3D Printing

Xiance Wang, Juan J. Hernandez, Guangzhe Gao, Jeffrey W. Stansbury, and Christopher N. Bowman*

Cite This: *Macromolecules* 2021, 54, 4042−4049 Read Online

ABSTRACT: Photocurable thiol-norbornene resins featuring triazole-embedded norbornene monomers were developed, and the photopolymerized networks showed good to superior ductility in the glassy state with elongation-at-break ranging from 130 to 290% and tensile toughness as high as 57 MJ/m^3, demonstrating the value of triazoles in forming tough, glassy networks. Retained ductility was observed with two of the triazole/thiol-norbornene networks after physical aging at ambient temperature for 24 h, presumably due to mechanical rejuvenation under uniaxial straining, as the elongation-at-break of one of the networks decreased only to 170 from 290%, while the elongation-at-break of the other network remained the same. Though substantial embrittlement was observed for both networks after an even more extended time of physical aging, the prolonged ductility observed here was not previously seen with the poly(triazole) glassy networks. Finally, one of the triazole/thiol-norbornene resins developed here was successfully applied for fabricating three-dimensional (3D) structures in high precision using stereolithography-based 3D printing, highlighting the robustness of the thiol-norbornene photopolymerization.

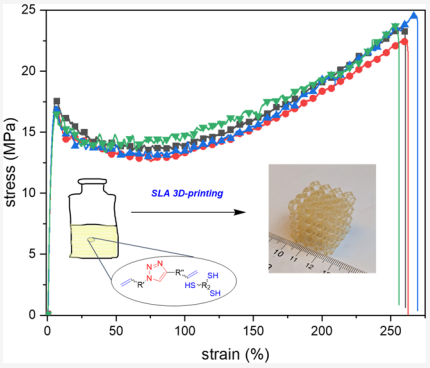

INTRODUCTION

Photopolymers are pervasive in daily life with applications spanning from coatings, adhesives, and dental restoratives to microelectronic photoresists.[1] One rapidly expanding area for photopolymerized materials is in additive manufacturing, commonly referred to as three-dimensional (3D) printing,[2,3] where photopolymerization-based technologies are frequently applied to rapidly convert liquid resins into solid polymeric objects with complex and, more often than not, conventionally unmoldable geometries.

With the ever-growing applications of photopolymerization-based technologies comes the simultaneous demand for photopolymers with exceptional mechanical performance and utility.[4] Currently, industrial applications primarily rely on photoinitiated chain-growth polymerizations of multifunctional (meth)acrylate or epoxy monomers to form cross-linked glassy thermosets, due to their rapid photocuring kinetics, the wide selection of commercially available monomers, and often, the mechanical stiffness/strength of the photopolymers formed.[5,6] However, there are intrinsic limitations with chain-growth polymerizations. First, chain-growth polymerizations lead to limited maximum conversions due to early gelation/vitrification,[7] and the unreacted monomers are potentially leachable potentially constituting an environmental and/or health issue.[8] Further, there is often a substantial buildup of shrinkage stress during chain-growth polymerizations, especially in free-radical polymerizations of multifunctional (meth)acrylates, and the high shrinkage stress is detrimental, particularly in additive manufacturing applications, leading to premature failure of the material or to de-bonding between layers or between a photopolymerized material and the underlying substrate.[9−11] Finally, (meth)acrylate-based glassy thermosets are known to be brittle with quite limited elongations-at-break, generally making them unsuitable for applications where large deformation or high toughness is needed.[12,13]

One popular approach to toughening brittle, glassy materials has been to integrate a rubbery phase into the matrix, also known as rubber toughening. Either nonreactive thermoplastics or reactive block copolymers have been incorporated into epoxy networks to afford glassy thermosets with improved mechanical performance.[14,15] Another approach is to employ secondary chemistries to form either a hybrid network or an interpenetrating network.[16] For example, Wei et al. showed that glassy networks based on photocurable thiol-ene-acrylate ternary systems exhibit enhanced energy absorption at room temperature.[17] Similarly, Beigi et al. investigated thiol-ene-methacrylate ternary resins for dental restorative composites and found that the fracture toughness was enhanced by

Received: January 11, 2021
Revised: April 7, 2021
Published: April 23, 2021

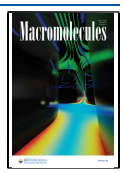

https://doi.org/10.1021/acs.macromol.1c00047
Macromolecules 2021, 54, 4042−4049

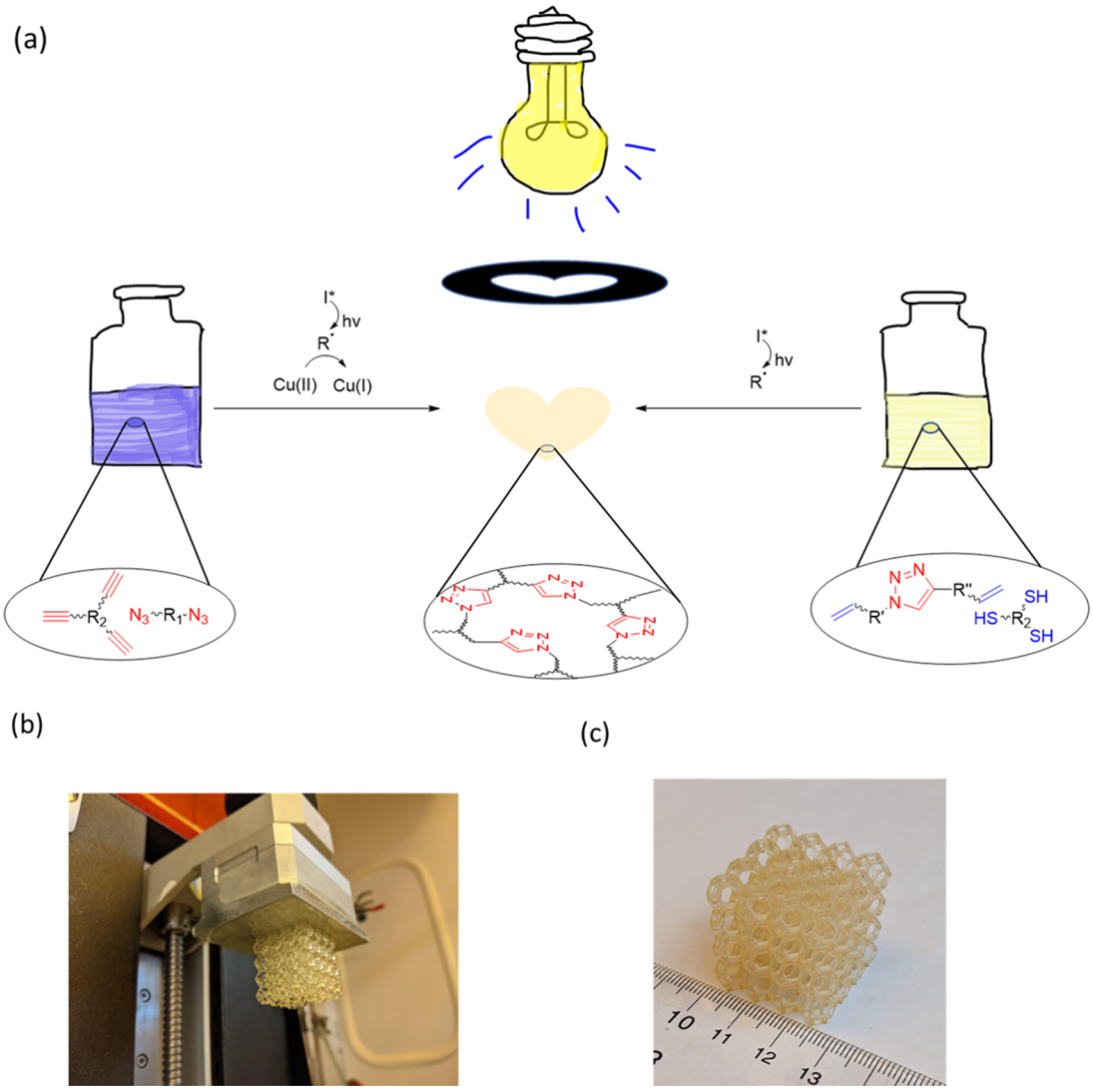

Figure 1. (a) Schematic representation of the thiol-ene photopolymerization as an alternative approach to forming poly(triazole) networks using triazole-containing monomers. (b) Bottom-up platform for stereolithography (SLA) 3D printing. (c) Sample print of a 27 × 27 × 27 mm^3 lattice cube based on triazole/thiol-norbornene photopolymerization.

increasing the weight percentage of the thiol-ene component.[18] Interpenetrating polymer networks (IPN) consisting of two or more interwoven polymeric matrixes are an emerging approach to enhancing the mechanical properties of photocured polymeric materials.[19,20] Jansen et al. prepared both IPNs and semi-IPNs based on epoxy/methacrylate systems and observed synergistic toughening.[21] Other approaches to toughening photocured thermosetting materials include incorporating chain transfer agents in dimethacrylate-based thermosets to form more homogeneous networks,[22,23] applying a second-stage thermal curing to affect the dynamic covalent exchange of blocked amine-isocyanate bond with primary amines/alcohols to reorganize the photocured polymer networks,[24,25] and adding inorganic nanoparticles or pre-formed organic particles as toughening additives.[26−31]

"Click" chemistries,[32−34] among them notably the copper-catalyzed azide−alkyne cycloaddition (CuAAC) reaction[35−40] and thiol-X reactions,[41−44] are a drastically different, and yet intriguing approach to preparing tough photopolymers. Hoyle and co-workers prepared thiourethane-based thiol-ene networks that showed good impact strength and crack resistance upon bending,[45] while Griesser and co-workers showed that thiol-yne-based glassy network exhibited about 5 times higher impact strength in comparison to diacrylate-based networks.[46] Unlike (meth)acrylate-based (radical) or many epoxy-based (cationic) polymerizations, polymerizations based on click chemistries are step-growth processes, through which both a high maximum conversion and low shrinkage stress are achieved due to delayed gelation. Further, the material properties are readily tuned by modifying the monomer structures and the overall composition.

Recently, it has been shown that photoinitiated CuAAC polymerizations often form glassy networks exhibiting superior toughness with excellent shape memory characteristics.[47,48] The monomers investigated, however, also had urethane moieties, which form tough networks due to the energy-dissipating character of the hydrogen bonds. Ether-based CuAAC polymeric foams developed by Alzahrani et al. exhibited higher toughness compared with epoxy/amine-based foams of the similar glass-transition temperature.[49] Inspired by the thiol-ene approach demonstrated by Song et al.,[47] and motivated by the chemical/thermal stability of

https://doi.org/10.1021/acs.macromol.1c00047
Macromolecules 2021, 54, 4042−4049

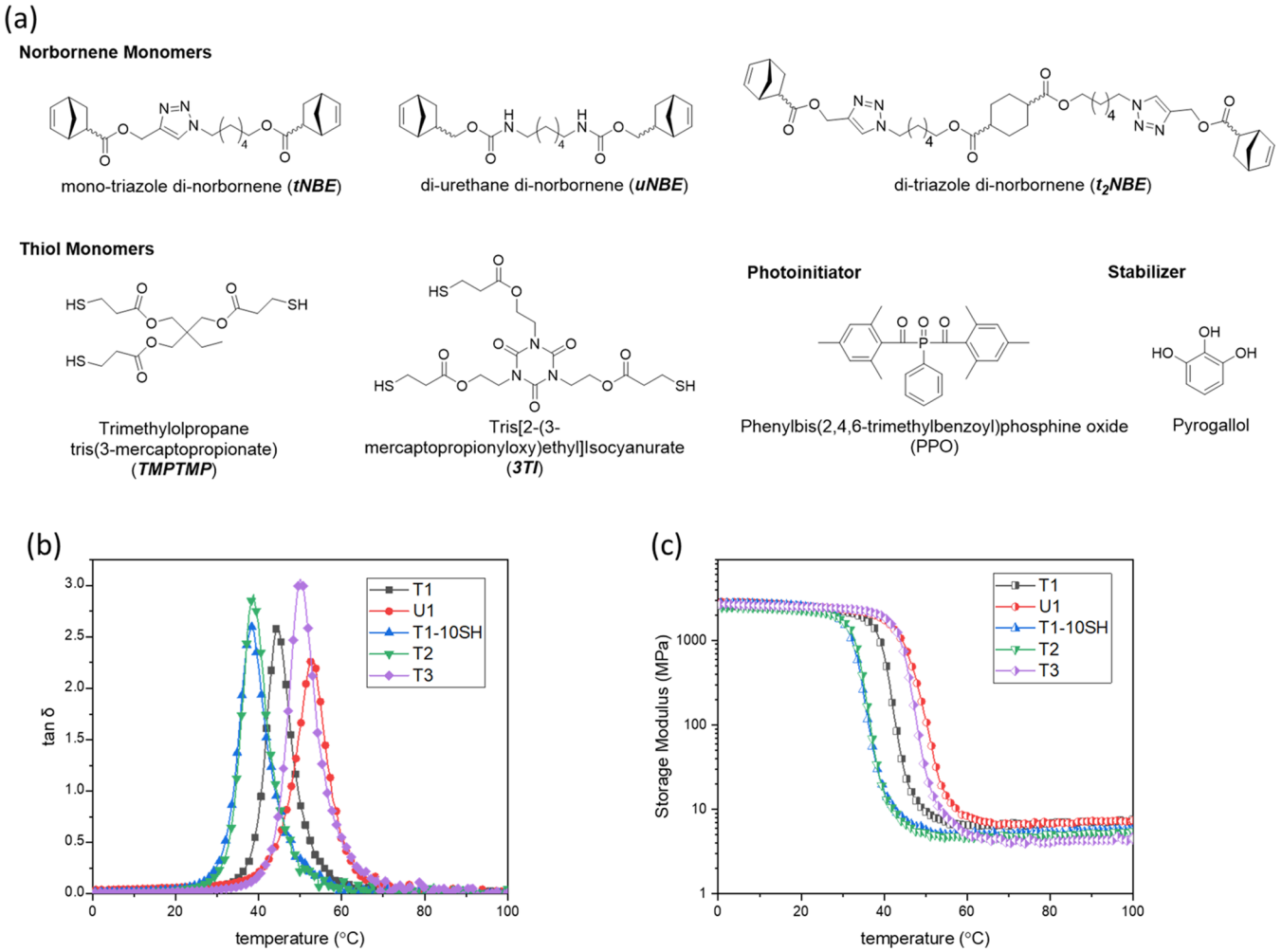

Figure 2. (a) Chemical structures of the monomers and other components used in this study. (b) Plots of tan δ vs temperature for the thiol-norbornene polymer networks investigated. (c) Plots of storage modulus vs temperature for the thiol-norbornene polymer networks investigated. All resins were composed of 1 wt % PPO and 0.05 wt % pyrogallol and were cured with 2 mW/cm^2 visible light with a wavelength of 400−500 nm at ambient temperature and then postcured overnight in an 80 °C oven. Representative curves are presented as the second cycle in the dynamic mechanical analysis (DMA). **T1** = ***tNBE/TMPTMP*** (3:2); **U1** = ***uNBE/TMPTMP*** (3:2); **T1−10SH** = ***tNBE/TMPTMP*** (3:2.2); **T2** = ***t$_2$NBE/TMPTMP*** (3:2); and **T3** = ***t$_2$NBE/3TI*** (3:2).

Table 1. Mechanical Properties of the Thiol-Norbornene Networks Obtained from Dynamical Mechanical Analysis (DMA) (Figure 2b,c) and Tensile Testing (Figure 3)[a]

	T1	U1	T1−10SH	T2	T3
T_g (°C)	43 ± 1	53 ± 1	38 ± 1	39 ± 1	50 ± 1
storage modulus@23 °C (GPa)	2.4 ± 0.1	2.5 ± 0.1	2.5 ± 0.2	2.1 ± 0.1	2.5 ± 0.1
rubbery modulus@T_g + 40 °C (MPa)	6.9 ± 0.1	7.1 ± 0.4	5.7 ± 0.2	4.7 ± 0.2	4.1 ± 0.2
network crosslink density[b] (mmol/cm^3)	0.82	0.82	0.69	0.57	0.48
triazole/urethane concentration (mmol/g)	1.40	2.79	1.35	1.90	1.76
tensile yield stress (MPa)	31 ± 2	36 ± 2	17 ± 1	21 ± 1	40 ± 2
tensile Young's modulus (MPa)	1040 ± 30	980 ± 20	720 ± 40	790 ± 40	1190 ± 10
tensile toughness (MJ/m^3)	29 ± 2	29 ± 2	43 ± 1	57 ± 3	46 ± 4
tensile elongation-at-break (%)	130 ± 10	100 ± 10	260 ± 10	290 ± 10	170 ± 10

[a]Errors listed are the standard deviation from multiple measurements (three runs for the DMA and four runs for the tensile testing). [b]Calculated based on the affine theory of rubbery elasticity.[52,53] **T1** = ***tNBE/TMPTMP*** (3:2); **U1** = ***uNBE/TMPTMP*** (3:2); **T1−10SH** = ***tNBE/TMPTMP*** (3:2.2); **T2** = ***t$_2$NBE/TMPTMP*** (3:2); and **T3** = ***t$_2$NBE/3TI*** (3:2).

triazoles as well as their rich secondary interactions,[50] here, thiol-norbornene photopolymer networks, harnessing triazole-embedded norbornene monomers, are implemented to demonstrate the value of triazoles for forming glassy networks with high tensile toughness that are comparable to similar networks featuring urethane moieties. In addition, retained ductile behavior was observed in the triazole-based thiol-norbornene networks after physical aging at ambient temperature. Finally, taking advantage of the rapid photocuring kinetics of thiol-norbornene polymerizations, one of the

https://doi.org/10.1021/acs.macromol.1c00047
Macromolecules 2021, 54, 4042−4049

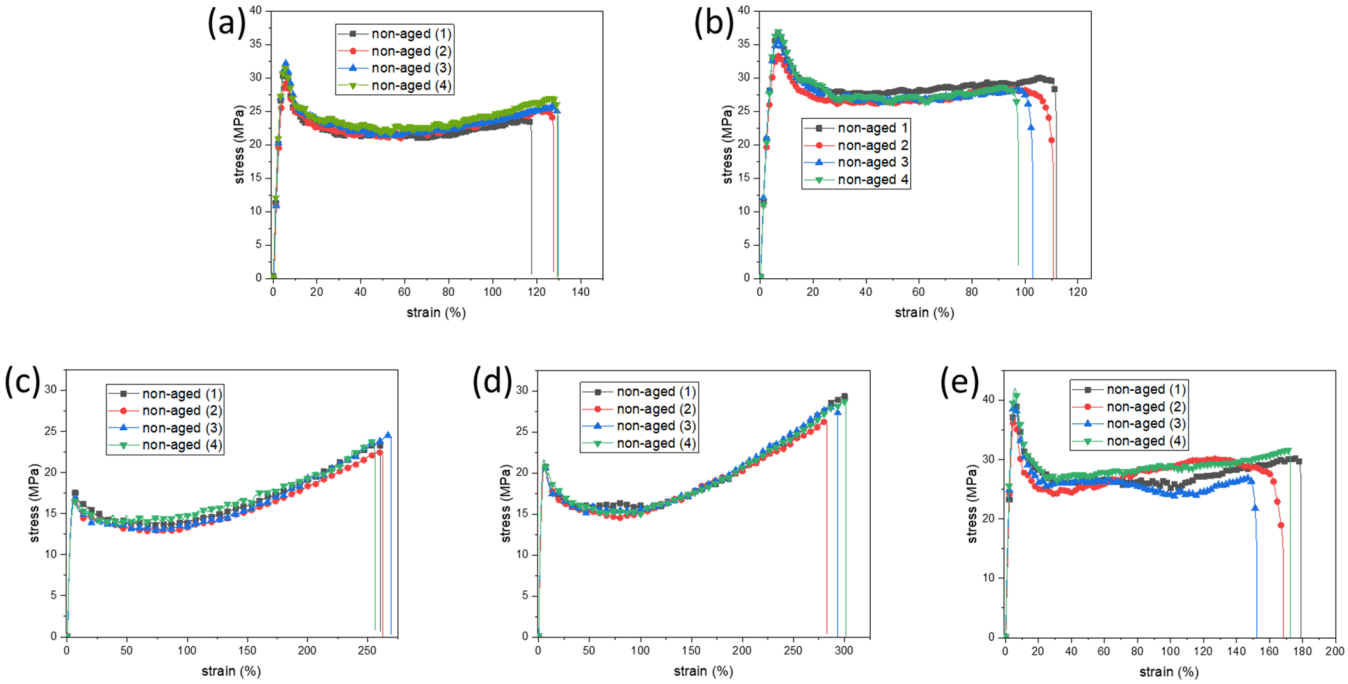

Figure 3. Tensile testing of the thiol-norbornene networks investigated: (a) **T1**, (b) **U1**, (c) **T1−10SH**, (d) **T2**, and (e) **T3**. Each specimen was kept at 80 °C before cooling at ambient temperature for 3 min prior to tensile testing with a strain rate of 6.7%/min. For each group of samples, four replicates were evaluated. **T1** = ***tNBE/TMPTMP*** (3:2); **U1** = ***uNBE/TMPTMP*** (3:2); **T1−10SH** = ***tNBE/TMPTMP*** (3:2.2); **T2** = ***t*$_2$*NBE/TMPTMP*** (3:2); and **T3** = *t*$_2$*NBE/3TI* (3:2).

triazole-based thiol-norbornene photopolymers was implemented to three-dimensional (3D) print objects with high precision.

■ RESULTS AND DISCUSSION

Thiol-ene photopolymer networks featuring multifunctional norbornene monomers tend to have high glass-transition temperatures (T_g) due to mobility restrictions.[51] Thus, two difunctional norbornene monomers were designed and synthesized with high overall yields (see the Supporting Information for the synthesis): one being a triazole-based di-norbornene (***tNBE***) and the other being a (di)urethane-based di-norbornene (***uNBE***) (see Figure 1a for the chemical structures). Photopolymerization of either the ***tNBE*** or the ***uNBE*** monomer, with a tri-thiol monomer, trimethylolpropane tris(3-mercaptopropionate) (***TMPTMP***) under visible light (400−500 nm) irradiation, proceeded smoothly, achieving maximum conversions within 30 s (For the photocuring kinetics, see Figure S1−S5, Supporting Information). Both the poly(triazole) network (**T1**) and the poly(urethane) network (**U1**) obtained after postcuring were glassy with storage moduli of 2.4 and 2.5 GPa, respectively, at ambient temperature (Figure 2c). The glass-transition temperature (T_g) of the **T1** network was about 10 °C lower than that of the **U1** network (43 vs 53 °C) (Figure 2b) despite the molecular similarity, which was attributed to the lower concentration of the triazole moieties in the **T1** network as compared with that of the urethane moieties in the **U1** network (Table 1).

Tensile testing showed that the **T1** and the **U1** networks exhibited similar ductility (Figure 3), both with five strain amplitude regimes: (i) an elastic regime where stress grows linearly with (low) strain (<2%); (ii) an "anelastic" regime where stress slowly peaked at the so-called "yield point"; (iii) a "strain softening" regime where the stress dropped with increasing strain; (iv) a plateaued plastic flow regime at nearly constant stress; and (v) a "strain hardening" regime where stress slightly increased at large deformation before rupture. The triazole-based **T1** network exhibited better elongation-at-break (130 vs 100%), while the urethane-based **U1** network showed higher yield stress (36 vs 31 MPa). Both types of networks, however, exhibited identical tensile toughness (29 MJ/m^3 for both networks, which is less than half of the value observed by Song et al.[47] with their urethane-based CuAAC network highlighting the synergistic effects of triazoles and urethanes in their system), while having similar Young's moduli (Table 1).

To enhance further the ductility of the poly(triazole) network, an off-stoichiometric system with excess thiol groups was investigated as a way to reduce both the crosslinking density and the glass-transition temperature, which would favor postyield plastic flow and lead to tougher networks. Having 10 mol % excess of the thiol groups (of ***TMPTMP***) in comparison to the norbornene groups (of ***tNBE***), with the resulting network denoted as **T1−10SH**, reduced T_g by about 5 °C compared to the **T1** network. Despite the slightly lower T_g (38 °C), the **T1−10SH** network was still glassy at ambient temperature with a storage modulus of about 2.5 GPa (Figure 2c). Calculations based on the rubbery modulus of the **T1−10SH** network showed a 16% decrease in the crosslink density. Tensile testing showed that the Young's modulus of **T1−10SH** was about 30% lower than that of **T1**, while the elongation-at-break approximately doubled (260 vs 130%) with more pronounced strain hardening of the **T1−10SH** network at large deformation (>100%). Overall, the lower T_g and the lower crosslink density of the **T1−10SH** network improved its tensile toughness by about 50% in comparison to the **T1** network (Table 1).

https://doi.org/10.1021/acs.macromol.1c00047
Macromolecules 2021, 54, 4042−4049

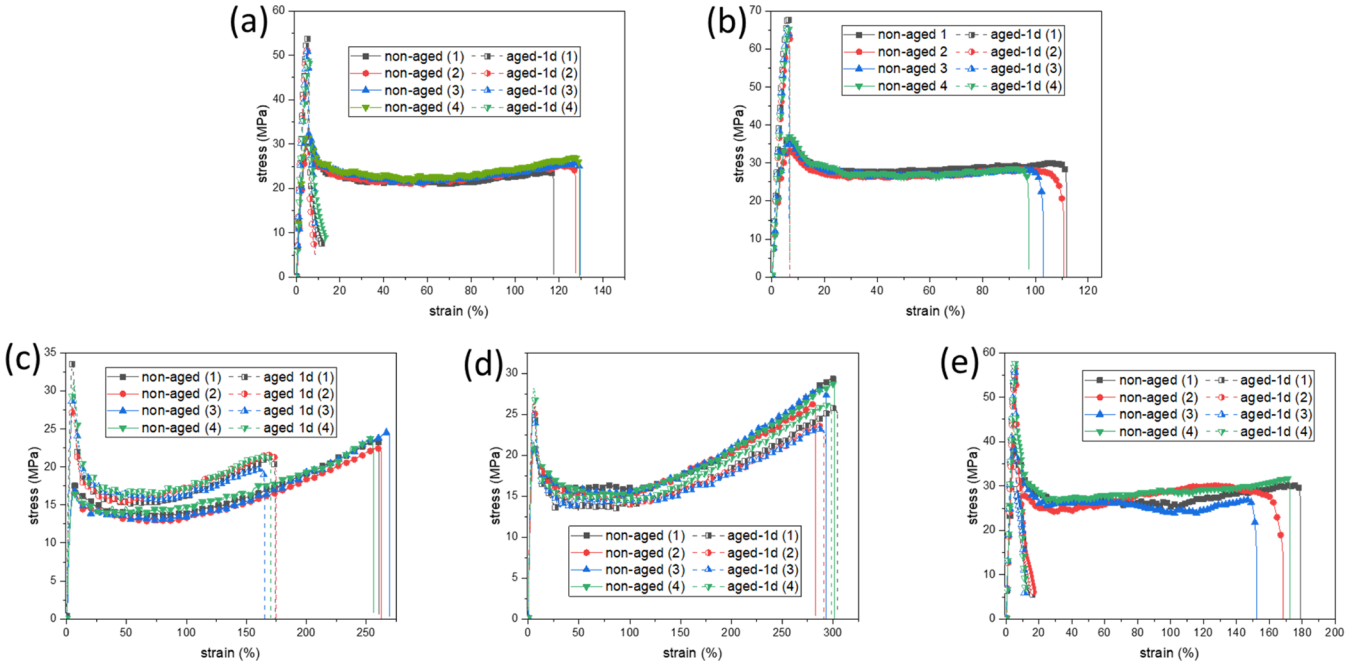

Figure 4. Physical aging effects on the tensile testing of the thiol-norbornene networks investigated: (a) **T1**, (b) **U1**, (c) **T1−10SH**, (d) **T2**, and (e) **T3** networks. The nonaged samples are represented by solid lines and filled symbols, while the aged (1 day at ambient temperature) samples are represented by dashed lines and half-filled symbols. Four measurements are shown for each group of samples. **T1** = ***tNBE/TMPTMP*** (3:2), **U1** = ***uNBE/TMPTMP*** (3:2), **T1−10SH** = ***tNBE/TMPTMP*** (3:2.2), **T2** = ***t_2NBE/TMPTMP*** (3:2), and **T3** = ***t_2NBE/3TI*** (3:2).

Table 2. Mechanical Properties of the Thiol-Norbornene Networks Before and After Being Aged at Ambient Temperature for 24 h as Determined from Tensile Testing (Figures 3 and 4)[a]

		T1	U1	T1−10SH	T2	T3
tensile yield stress (MPa)	nonaged	31 ± 2	36 ± 2	17 ± 1	21 ± 1	40 ± 2
	aged	51 ± 2	66 ± 2	31 ± 2	27 ± 1	57 ± 1
tensile Young's modulus (MPa)	nonaged	1040 ± 30	980 ± 20	720 ± 40	790 ± 40	1190 ± 10
	aged	1420 ± 80	1490 ± 40	1060 ± 40	950 ± 10	1440 ± 40
tensile toughness (MJ/m^3)	nonaged	29 ± 2	29 ± 2	43 ± 1	57 ± 3	46 ± 4
	aged	2.0 ± 0.1	2.8 ± 0.1	31 ± 1	52 ± 3	2.9 ± 0.2
elongation-at-break (%)	nonaged	130 ± 10	100 ± 10	260 ± 10	290 ± 10	170 ± 10
	aged	6.5 ± 0.4	6.7 ± 0.2	170 ± 10	290 ± 10	8.5 ± 0.7

[a]Errors listed are the standard deviation from four measurements for each group of samples. **T1** = ***tNBE/TMPTMP*** (3:2); **U1** = ***uNBE/TMPTMP*** (3:2); **T1−10SH** = ***tNBE/TMPTMP*** (3:2.2); **T2** = ***t_2NBE/TMPTMP*** (3:2); and **T3** = ***t_2NBE/3TI*** (3:2).

To form triazole/thiol-norbornene networks with higher strength and higher tensile toughness, a di-triazole di-norbornene monomer (***t_2NBE***, see Figure 1a for the chemical structure) was designed and synthesized (for the synthesis, see the Supporting Information), featuring a cyclohexane core, as cyclohexane moieties were shown to reduce the viscosity of the resins while enhancing the impact strength of the polymers due to its capacity for ring flipping at ambient temperature.[54,55] Photopolymerization of ***t_2NBE*** and ***TMPTMP*** afforded a glassy network (**T2**) with a glass-transition temperature of 39 °C and storage modulus (at ambient temperature) of 2.1 GPa (Figure 2b,c). Despite the higher triazole concentration, the **T2** network exhibited both a lower Young's modulus (790 vs 1040 MPa) and lower yield stress (21 vs 31 MPa) in comparison to the ***tNBE***-based **T1** network, which was attributed to the low crosslink density of the **T2** network (Table 1) due to the more extended molecular structure of ***t_2NBE*** (Figure 1a). Consequently, superior ductility of the **T2** network was observed (Figure 3d), with elongation-at-break and tensile toughness increased by 120 and 97% (Table 1), respectively, in comparison to the **T1** network. With the superior ductility of the **T2** network, it was anticipated that replacing the flexible tri-thiol ***TMPTMP*** with a rigid thiol monomer would form a high-strength network at the cost of some of the ductility. Photocuring of ***t_2NBE*** and tris[2-(3-mercaptopropionyloxy)ethyl] isocyanurate (***3TI***, a tri-thiol monomer with a rigid isocyanurate core) produced a glassy network (**T3**) with a T_g of 50 °C, and the yield stress almost doubled compared with the **T2** network (40 vs 21 MPa), while the Young's modulus increased to 1190 from 790 MPa (Table 1). The **T3** network still showed high ductility (Figure 3e), however, with the elongation-at-break reaching about 170%, while the tensile toughness decreased by one-fifth in comparison to the **T2** network (46 vs 57 MJ/m^3). Overall, increasing the triazole concentration did not enhance the strength or modulus of the **T2** network due to the counter effect of the reduced crosslink density, while the higher triazole concentration and the reduced crosslink density did significantly improve the tensile toughness of the **T2** network. Further, higher strength and improved tensile toughness were

https://doi.org/10.1021/acs.macromol.1c00047
Macromolecules 2021, 54, 4042−4049

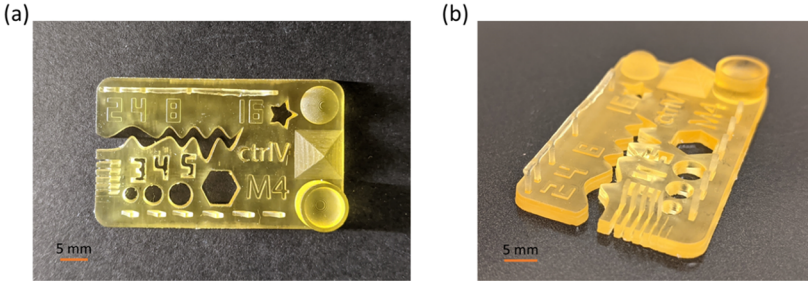

Figure 5. Sample 3D print with a series of challenging features: (a) top view and (b) side view.

achieved with the **T3** network by combining the higher triazole concentration and the reduced crosslink density with more rigid monomer backbones.

Glassy materials quenched below their glass-transition temperature exist in a nonequilibrium state with frozen-in excess free volume, and their relaxation toward the equilibrium state is referred to as physical aging.[56−58] For glassy polymer networks, the excess free volume and the enthalpy decrease upon physical aging through repositioning of the polymer segments, which leads to a corresponding change of the mechanical properties. Previously, it was shown that the elongation-at-break of the urethane-based triazole glassy network decreased from 200% to less than 20% after 16 h of physical aging at ambient temperature, while the yield stress increased to 66 from 37 MPa.[47] Physical aging could be thermally reversed by heating the material above its glass-transition temperature, or as recently demonstrated by Sowan et al., physical aging of the triazole-based glassy networks could also be photochemically reversed through photoinduced dynamic covalent-bond exchange.[59] To investigate the physical aging effect on the glassy thiol-norbornene networks, tensile testing was conducted on the samples aged at ambient temperature and compared with the pristine (nonaged) samples. For the **T1**, **U1**, and **T3** networks, significant embrittlement was observed after aging at ambient temperature for as little as 24 h with a sharp increase of the yield stress and decrease in the elongation-at-break (Figure 4 and Table 2). For the **T1−10SH** network, however, high ductility was observed despite the increase of the yield stress from 17 to 31 MPa (Figure 4c), with the elongation-at-break decreased only to 170 from 260% after 24 h of aging at ambient temperature. For the **T2** network, there was only a slight increase of both the yield stress (21−27 MPa) and the Young's modulus (790−950 MPa), while the elongation-at-break was almost identical to that of the nonaged samples (Figure 4d and Table 1). The ductile behavior of the aged **T1−10SH** and **T2** networks was attributed to the erasure of aging by the applied stresses under uniaxial straining, or the so-called "mechanical rejuvenation,"[56] and their (relatively) low glass-transition temperatures are potentially the reason that the mechanical rejuvenation was observed only with the **T1−10SH** and **T2** networks. In spite of the almost identical glass-transition temperatures of **T1−10SH** and **T2**, the slight increase of the yield stress and the Young's modulus of the **T2** network after physical aging were indicative of an earlier onset of mechanical rejuvenation during uniaxial deformation as compared with the aged **T1−10SH** network, while the nearly complete retainment of elongation-at-break of the **T2** network indicated a larger extent of mechanical rejuvenation, both of which were likely promoted by the cyclohexane moieties with their ring flipping at room temperature.[54] Ultimately, substantial embrittlement was observed for both the **T1−10SH** network and the **T2** network with extended physical aging time, as the elongation-at-break of the **T1−10SH** network decreased to 58% after 7 days of physical aging and to 13% after 14 days of physical aging (Figure S11), while the elongation-at-break of the **T2** network decreased to 18% after 7 days of physical aging (Figure S12).

Of the two triazole/thiol-norbornene networks (**T1−10SH** and **T2**) with the highest ductility, the **T1−10SH** network was chosen for implementation in stereolithography-based (SLA)[60,61] 3D printing due to the ease of resin preparations (see theSupporting Information). SLA 3D printing is a layer-by-layer process based on vat photopolymerization technologies, where 3D objects are fabricated from liquid resins through photoinduced vitrification. Taking advantage of the fast photocuring kinetics of the thiol-norbornene polymerization and the improved mechanical performance of the poly(triazole) networks, an otherwise unmoldable 3D object (the lattice cube, Figure 1c) was fabricated using the **T1−10SH** resin, and structures with challenging features (overhangs, bridges, holes of different sizes and shapes, and different surfaces) were also successfully printed with high precision (Figures 5 and S11, Supporting Information), highlighting the robustness of the photocurable triazole/thiol-norbornene networks for customizable 3D printing of complex structures with great mechanical properties.

■ CONCLUSIONS

We have developed photocurable thiol-norbornene-based poly(triazole) networks that not only demonstrated the value of triazole moieties in forming glassy networks with high ductility and high tensile toughness but were also successfully applied as photocurable resins for SLA-based 3D printing to fabricate complex objects with high precision. This approach, in contrast to the previous CuAAC approach utilizing azide−alkyne functional monomers, is safer, potentially eliminates copper, and leads to improved spatial control, which facilitated poly(triazole) networks being applied to 3D printing as high ductility and high tensile toughness are desirable properties for 3D-printed materials. Divergent physical aging results (embrittlement vs retained ductility) were observed with different triazole/thiol-norbornene networks, and the retained ductility of the networks with relatively low T_g was attributed to "mechanical rejuvenation," though substantial embrittlement was observed after the more extended physical aging time (>7 days). One drawback of the triazole/thiol-norbornene glassy networks reported here is their relatively low glass-transition temperatures.

https://doi.org/10.1021/acs.macromol.1c00047
Macromolecules 2021, 54, 4042−4049

■ ASSOCIATED CONTENT

Supporting Information

The Supporting Information is available free of charge at https://pubs.acs.org/doi/10.1021/acs.macromol.1c00047.

Synthetic routes and additional characterization; related characterization results including ^{1}H NMR, FT-IR, DMA, and tensile tests; and additional experimental details and related characterization results (PDF)

■ AUTHOR INFORMATION

Corresponding Author

Christopher N. Bowman − *Department of Chemical and Biological Engineering, University of Colorado Boulder, Boulder, Colorado 80303, United States; Materials Science and Engineering Program, University of Colorado Boulder, Boulder, Colorado 80309, United States;* orcid.org/0000-0001-8458-7723; Email: christopher.bowman@colorado.edu

Authors

Xiance Wang − *Department of Chemical and Biological Engineering, University of Colorado Boulder, Boulder, Colorado 80303, United States*

Juan J. Hernandez − *Department of Chemical and Biological Engineering, University of Colorado Boulder, Boulder, Colorado 80303, United States*

Guangzhe Gao − *Materials Science and Engineering Program, University of Colorado Boulder, Boulder, Colorado 80309, United States*

Jeffrey W. Stansbury − *Department of Chemical and Biological Engineering, University of Colorado Boulder, Boulder, Colorado 80303, United States; Department of Craniofacial Biology, School of Dental Medicine, University of Colorado Denver, Aurora, Colorado 80045, United States;* orcid.org/0000-0003-1880-005X

Complete contact information is available at: https://pubs.acs.org/10.1021/acs.macromol.1c00047

Notes

The authors declare no competing financial interest.

■ ACKNOWLEDGMENTS

The authors acknowledge the National Science Foundation (CHE 1808484) for providing funding for this research.

■ REFERENCES

(1) Crivello, J. V.; Reichmanis, E. Photopolymer Materials and Processes for Advanced Technologies. *Chem. Mater.* **2014**, *26*, 533−548.

(2) Lipson, H.; Kurman, M. *Fabricated: The New World of 3D Printing*; Wiley: Indianapolis, 2013.

(3) Tumbleston, J. R.; Shirvanyants, D.; Ermoshkin, N.; Janusziewicz, R.; Johnson, A. R.; Kelly, D.; Chen, K.; Pinschmidt, R.; Rolland, J. P.; Ermoshkin, A.; Samulski, E. T.; DeSimone, J. M. Continuous Liquid Interface Production of 3D Objects. *Science* **2015**, *347*, 1349−1352.

(4) Meijer, H. E. H.; Govaert, L. E. Mechanical Performance of Polymer Systems: The Relation between Structure and Properties. *Prog. Polym. Sci.* **2005**, *30*, 915−938.

(5) Jacobine, A. T. *Polymerization Mechanisms. Radiation Curing in Polymer Science and Technology*; Fouassier, J. P.; Rebek, J. F., Eds.; Elsevier, Science: New York, 1993; pp 3311−3319.

(6) Bulut, U.; Crivello, J. V. Investigation of the Reactivity of Epoxide Monomers in Photoinitiated Cationic Polymerization. *Macromolecules* **2005**, *38*, 3584−3595.

(7) Kloosterboer, J. G.; Lijten, G. F. C. M. *The Influence of Vitrification on the Formation of Densely Crosslinked Networks Using Photopolymerization. Biological and Synthetic Polymer Networks*; Kramer, O., Ed.; Springer: Dordrecht, 1988; pp 345−355.

(8) Staffanou, R. S.; Hembree, J. H., Jr.; Rivers, J. A.; Myers, M. L.; Kilgore, J. K. Leakage Study of Three Esthetic Veneering Materials. *J. Prosthet. Dent.* **1985**, *54*, 204−206.

(9) Lu, H.; Stansbury, J. W.; Bowman, C. N. Impact of Curing Protocol on Conversion and Shrinkage Stress. *Dent. Mater.* **2004**, *20*, 979−986.

(10) Mantri, S. P.; Mantri, S. S. Management of Shrinkage Stresses in Direct Restorative Light-Cured Composites: A Review. *J. Esthet. Restor. Dent.* **2013**, *25*, 305−313.

(11) Verzijden, C. W.; Feilzeri, A. J.; Creugers, N. H. J.; Davidson, C. L. The Influence of Polymerization Shrinkage of Resin Cements on Bonding to Metal. *J. Dent. Res.* **1992**, *71*, 410−413.

(12) Matsushige, K.; Radcliffe, S. V.; Baer, E. The Mechanical Behavior of Poly(methyl methacrylate) under Pressure. *J. Polym. Sci., Part B: Polym. Phys.* **1976**, *14*, 703−721.

(13) Ishikawa, M.; Ogawa, H.; Narisawa, I. Brittle Fracture in Glassy Polymers. *J. Macromol. Sci., Part B: Phys.* **1981**, *19*, 421−443.

(14) Rebizant, V.; Venet, A.-S.; Tournilhac, F.; Girard-Reydet, E.; Navarro, C.; Pascault, J.-P.; Leibler, L. Chemistry and Mechanical Properties of Epoxy-Based Thermosets Reinforced by Reactive and Nonreactive SBMX Block Copolymers. *Macromolecules* **2004**, *37*, 8017−8027.

(15) Chikhi, N.; Fellahi, S.; Bakar, M. Modification of Epoxy Resin Using Reactive Liquid (ATBN) Rubber. *Eur. Polym. J.* **2002**, *38*, 251−264.

(16) Sperling, L. H. *Interpenetrating Polymer Networks and Related Materials*; Plenum Press: New York, 1981.

(17) Wei, H.; Senyurt, A. F.; Jönsson, S.; Hoyle, C. E. Photopolymerization of Ternary Thiol−Ene/Acrylate Systems: Film and Network Properties. *J. Polym. Sci., Part A: Polym. Chem.* **2007**, *45*, 822−829.

(18) Beigi, S.; Yeganeh, H.; Atai, M. Evaluation of Fracture Toughness and Mechanical Properties of Ternary Thiol−Ene−Methacrylate Systems as Resin Matrix for Dental Restorative Composites. *Dent. Mater.* **2013**, *29*, 777−787.

(19) Matsuda, T.; Kawakami, R.; Namba, R.; Nakajima, T.; Gong, J. P. Mechanoresponsive Self-growing Hydrogels Inspired by Muscle Training. *Science* **2019**, *363*, 504−508.

(20) Lu, H.-F.; Wang, M.; Chen, X.-M.; Lin, B.-P.; Yang, H. Interpenetrating Liquid-Crystal Polyurethane/Polyacrylate Elastomer with Ultrastrong Mechanical Property. *J. Am. Chem. Soc.* **2019**, *141*, 14364−14369.

(21) Jansen, B. J. P.; Rastogi, S.; Meijer, H. E. H.; Lemstra, P. J. Rubber-Modified Glassy Amorphous Polymers Prepared via Chemically Induced Phase Separation. 4. Comparison of Properties of Semi- and Full-IPNs, and Copolymers of Acrylate−Aliphatic Epoxy Systems. *Macromolecules* **1999**, *32*, 6290−6297.

(22) Gorsche, C.; Griesser, M.; Gescheidt, G.; Moszner, N.; Liska, R. *β*-Allyl Sulfones as Addition−Fragmentation Chain Transfer Reagents: A Tool for Adjusting Thermal and Mechanical Properties of Dimethacrylate Networks. *Macromolecules* **2014**, *47*, 7327−7336.

(23) Gorsche, C.; Seidler, K.; Knaack, P.; Dorfinger, P.; Koch, T.; Stampfl, J.; Moszner, N.; Liska, R. Rapid Formation of Regulated Methacrylate Networks Yielding Tough Materials for Lithography-based 3D Printing. *Polym. Chem.* **2016**, *7*, 2009−2014.

(24) Rolland, J. P.; Chen, K.; Poelma, J.; Goodrich, J.; Pinschmidt, R.; DeSimone, J. M.; Robeson, L. M. Methods of producing three-dimensional objects from materials having multiple mechanisms of hardening. U.S. Patent US9676963, 2017.

(25) Rolland, J. P.; Chen, K.; Poelma, J.; Goodrich, J.; Pinschmidt, R.; DeSimone, J. M.; Robeson, L. M. Methods of producing

polyurethane three-dimensional objects from materials having multiple mechanisms of hardening. U.S. Patent US9598606, 2017.
(26) Bhuniya, S.; Adhikari, B. Toughening of Epoxy Resins by Hydroxy-Terminated, Silicon-Modified Polyurethane Oligomers. *J. Appl. Polym. Sci.* **2003**, *90*, 1497−1506.
(27) Sangermano, M.; Naguib, M.; Messori, M. Fracture Toughness Enhancement of UV-Cured Epoxy Coatings Containing Al2O3 Nanoparticles. *Macromol. Mater. Eng.* **2013**, *298*, 1184−1189.
(28) Marouf, B. T.; Pearson, R. A.; Bagheri, R. Anomalous Fracture Behavior in an Epoxy-Based Hybrid Composite. *Mater. Sci. Eng., A* **2009**, *515*, 49−58.
(29) Jingqiang, S.; Zhang, Y.; Qiu, J.; Kuang, J. Core-Shell Particles with an Acrylate Polyurethane Core as Tougheners for Epoxy Resins. *J. Mater. Sci.* **2004**, *39*, 6383−6384.
(30) He, J.; Raghavan, D.; Hoffman, D.; Hunston, D. The Influence of Elastomer Concentration on Toughness in Dispersions Containing Preformed Acrylic Elastomeric Particles in an Epoxy Matrix. *Polymer* **1999**, *40*, 1923−1933.
(31) Rey, L.; Poisson, N.; Maazouz, A.; Sautereau, H. Enhancement of Crack Propagation Resistance in Epoxy Resins by Introducing Poly(dimethylsiloxane) Particles. *J. Mater. Sci.* **1999**, *34*, 1775−1781.
(32) Kolb, H. C.; Finn, M. G.; Sharpless, K. B. Click Chemistry: Diverse Chemical Function from a Few Good Reactions. *Angew. Chem., Int. Ed.* **2001**, *40*, 2004−2021.
(33) Xi, W.; Scott, T. F.; Kloxin, C. J.; Bowman, C. N. Click Chemistry in Materials Science. *Adv. Funct. Mater.* **2014**, *24*, 2572−2590.
(34) Nandivada, H.; Jiang, X.; Lahann, J. Click Chemistry: Versatility and Control in the Hands of Materials Scientists. *Adv. Mater.* **2007**, *19*, 2197−2208.
(35) Rostovtsev, V. V.; Green, L. G.; Fokin, V. V.; Sharpless, K. B. A Stepwise Huisgen Cycloaddition Process: Copper(I)-Catalyzed Regioselective "Ligation" of Azides and Terminal Alkynes. *Angew. Chem., Int. Ed.* **2002**, *41*, 2596−2599.
(36) Tornøe, C. W.; Christensen, C.; Meldal, M. Peptidotriazoles on Solid Phase: [1,2,3]-Triazoles by Regiospecific Copper(I)-Catalyzed 1,3-Dipolar Cycloadditions of Terminal Alkynes to Azides. *J. Org. Chem.* **2002**, *67*, 3057−3064.
(37) Adzima, B. J.; Tao, Y.; Kloxin, C. J.; DeForest, C. A.; Anseth, K. S.; Bowman, C. N. Spatial and Temporal Control of the Alkyne−Azide Cycloaddition by Photoinitiated Cu(II) Reduction. *Nat. Chem.* **2011**, *3*, 256−259.
(38) Gong, T.; Adzima, B. J.; Baker, N. H.; Bowman, C. N. Photopolymerization Reactions Using the Photoinitiated Copper (I)-Catalyzed Azide-Alkyne Cycloaddition (CuAAC) Reaction. *Adv. Mater.* **2013**, *25*, 2024−2028.
(39) Tasdelen, M. A.; Yilmaz, G.; Iskin, B.; Yagci, Y. Photoinduced Free Radical Promoted Copper(I)-Catalyzed Click Chemistry for Macromolecular Syntheses. *Macromolecules* **2012**, *45*, 56−61.
(40) Tasdelen, M. A.; Yagci, Y. Light-Induced Click Reactions. *Angew. Chem., Int. Ed.* **2013**, *52*, 5930−5938.
(41) Killops, K. L.; Campos, L. M.; Hawker, C. J. Robust, Efficient, and Orthogonal Synthesis of Dendrimers via Thiol-ene "Click" Chemistry. *J. Am. Chem. Soc.* **2008**, *130*, 5062−5064.
(42) Hoyle, C. E.; Bowman, C. N. Thiol−Ene Click Chemistry. *Angew. Chem., Int. Ed.* **2010**, *49*, 1540−1573.
(43) De, S.; Khan, A. Efficient Synthesis of Multifunctional Polymers via Thiol−Epoxy "Click" Chemistry. *Chem. Commun.* **2012**, *48*, 3130−3132.
(44) Nair, D. P.; Podgórski, M.; Chatani, S.; Gong, T.; Xi, W.; Fenoli, C. R.; Bowman, C. N. The Thiol-Michael Addition Click Reaction: A Powerful and Widely Used Tool in Materials Chemistry. *Chem. Mater.* **2014**, *26*, 724−744.
(45) Li, Q.; Zhou, H.; Wicks, D. A.; Hoyle, C. E. Thiourethane-Based Thiol-Ene High Tg Networks: Preparation, Thermal, Mechanical, and Physical Properties. *J. Polym. Sci., Part A: Polym. Chem.* **2007**, *45*, 5103−5111.
(46) Oesterreicher, A.; Gorsche, C.; Ayalur-Karunakaran, S.; Moser, A.; Edler, M.; Pinter, G.; Schlögl, S.; Liska, R.; Griesser, T. Exploring Network Formation of Tough and Biocompatible Thiol-yne Based Photopolymers. *Macromol. Rapid Commun.* **2016**, *37*, 1701−1706.
(47) Song, H. B.; Baranek, A.; Worrell, B. T.; Cook, W. D.; Bowman, C. N. Photopolymerized Triazole-Based Glassy Polymer Networks with Superior Tensile Toughness. *Adv. Funct. Mater.* **2018**, *28*, No. 1801095.
(48) McBride, M. K.; Gong, T.; Nair, D. P.; Bowman, C. N. Photo-Mediated Copper(I)-Catalyzed Azide-Alkyne Cycloaddition (CuAAC) "Click" Reactions for Forming Polymer Networks as Shape Memory Materials. *Polymer* **2014**, *55*, 5880−5884.
(49) Alzahrani, A. A.; Saed, M.; Yakacki, C. M.; Song, H. B.; Sowan, N.; Walston, J. J.; Shah, P. K.; McBride, M. K.; Stansbury, J. W.; Bowman, C. N. Fully Recoverable Rigid Shape Memory Foam Based on Copper-Catalyzed Azide−Alkyne Cycloaddition (CuAAC) Using a Salt Leaching Technique. *Polym. Chem.* **2018**, *9*, 121−130.
(50) Schulze, B.; Schubert, U. S. Beyond Click Chemistry − Supramolecular Interactions of 1,2,3-Triazoles. *Chem. Soc. Rev.* **2014**, *43*, 2522−2571.
(51) Carioscia, J. A.; Schneidewind, L.; O'Brien, C.; Ely, R.; Feeser, C.; Cramer, N.; Bowman, C. N. Thiol−Norbornene Materials: Approaches to Develop High Tg Thiol−Ene Polymers. *J. Polym. Sci., Part A: Polym. Chem.* **2007**, *45*, 5686−5696.
(52) Flory, P. J. Molecular Theory of Rubber Elasticity. *Polym. J.* **1985**, *17*, 1−12.
(53) Hill, L. W. Calculation of Crosslink Density in Short Chain Networks. *Prog. Org. Coat.* **1997**, *31*, 235−243.
(54) Yoon, W. J.; Hwang, S. Y.; Koo, J. M.; Lee, Y. J.; Lee, S. U.; Im, S. S. Synthesis and Characteristics of a Biobased High-Tg Terpolyester of Isosorbide, Ethylene Glycol, and 1,4-Cyclohexane Dimethanol: Effect of Ethylene Glycol as a Chain Linker on Polymerization. *Macromolecules* **2013**, *46*, 7219−7231.
(55) Park, S.-A.; Choi, J.; Ju, S.; Jegal, J.; Lee, K. M.; Hwang, S. Y.; Oh, D. X.; Park, J. Copolycarbonates of Bio-Based Rigid Isosorbide and Flexible 1,4-Cyclohexanedimethanol: Merits over Bisphenol-A Based Polycarbonates. *Polymer* **2017**, *116*, 153−159.
(56) Struik, L. C. E. *Physical Aging in Amorphous Polymers and Other Materials*; Elsevier: Amsterdam, 1978.
(57) Hutchinson, J. M. Relaxation Processes and Physical Aging. In *The Physics of Glassy Polymers*; Haward, R. N.; Young, R. J., Eds.; Springer: Dordrecht, 1997.
(58) Angell, C. A. K.; Ngai, L.; McKenna, G. B.; McMillan, P. F.; Martin, S. W. Relaxation in Glassforming Liquids and Amorphous Solids. *J. Appl. Phys.* **2000**, *88*, 3113−3157.
(59) Sowan, N.; Song, H. B.; Cox, L. M.; Patton, J. R.; Fairbanks, B. D.; Ding, Y.; Bowman, C. N. Light-Activated Stress Relaxation, Toughness Improvement, and Photoinduced Reversal of Physical Aging in Glassy Polymer Networks. *Adv. Mater.* **2020**, *33*, No. 2007221.
(60) Hull, C. W. Apparatus for Production of Three-dimensional Objects by Stereolithography. U.S. Patent US45753301986.
(61) Jacobs, P. F. *Rapid Prototyping and Manufacturing: Fundamentals of Stereolithography*; Society of Manufacturing Engineers, 1992.

https://doi.org/10.1021/acs.macromol.1c00047
Macromolecules 2021, 54, 4042−4049